Acta Crystallographica Section F
Structural Biology and Crystallization Communications
ISSN 1744-3091

Purification, crystallization and preliminary X-ray crystallographic studies of the *Mycobacterium tuberculosis* DNA gyrase CTD

Amélie Darmon,[a,b] Jérémie Piton,[c] Mélanie Roué,[a,b] Stéphanie Petrella,[a,b] Alexandra Aubry[d] and Claudine Mayer[a,b]*

[a]Unité de Microbiologie Structurale, Institut Pasteur, CNRS URA 2185, 25 Rue du Dr Roux, 75015 Paris, France, [b]University Paris Diderot, Sorbonne Paris Cité (Cellule Pasteur), 25 Rue du Dr Roux, 75015 Paris, France, [c]CNRS UPR9073 (affiliated with Université Paris Diderot, Sorbonne Paris Cité), Institut de Biologie Physico-Chimique, 13 Rue Pierre et Marie Curie, 75005 Paris, France, and [d]ER5, EA 1541, Laboratoire de Bactériologie-Hygiène, UPMC Université Paris 06, 91 Boulevard de l'Hôpital, 75013 Paris, France

Correspondence e-mail: mayer@pasteur.fr

Received 31 October 2011
Accepted 1 December 2011

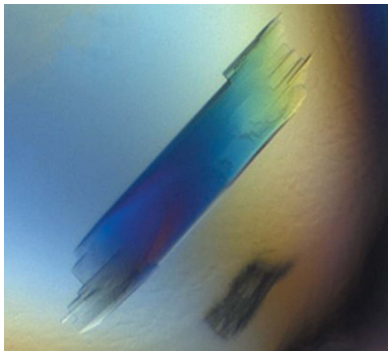

Mycobacterium tuberculosis DNA gyrase, a nanomachine involved in regulation of DNA topology, is the only type II topoisomerase present in this organism and hence is the sole target of fluoroquinolone in the treatment of tuberculosis. The C-terminal domain (CTD) of the DNA gyrase A subunit possesses a unique feature, the ability to wrap DNA in a chiral manner, that plays an essential role during the catalytic cycle. A construct of 36 kDa corresponding to this domain has been overproduced, purified and crystallized. Diffraction data were collected to 1.55 Å resolution. Cleavage of the N-terminal His tag was crucial for obtaining crystals. The crystals belonged to space group $P2_12_12_1$, with one molecule in the asymmetric unit and a low solvent content (33%). This is the first report of the crystallization and preliminary X-ray diffraction studies of a DNA gyrase CTD from a species that contains one unique type II topoisomerase.

1. Introduction

DNA gyrase and topoisomerase IV are type II topoisomerases that are found in almost all bacteria. These macromolecular assemblies, which are essential to cell life, are involved in the manipulation of DNA in biological processes such as replication and transcription. They resolve DNA topology by making double-strand breaks in the double helix (Champoux, 2001). DNA gyrase and topoisomerase IV are structurally and mechanistically related, but have acquired distinct biological functions during evolution (Champoux, 2001; Forterre & Gadelle, 2009). DNA gyrase is unique in introducing negative supercoils and facilitates DNA unwinding at replication forks, while topoisomerase IV has a specialized function in mediating the decatenation of interlocked daughter chromosomes (Champoux, 2001; Levine *et al.*, 1998).

Type II topoisomerases are heterotetrameric enzymes assembled from two subunits (A and B). Each subunit consists of two domains: the breakage-reunion domain (BRD) and the C-terminal domain (CTD) in the A subunit, and the ATPase and Toprim domains in subunit B (Schoeffler & Berger, 2008). DNA breakage occurs at the catalytic reaction core formed by the BRD and the Toprim domain. The CTD is responsible for the negative-supercoiling activity of DNA gyrase (Kampranis & Maxwell, 1996). The binding of the CTD to DNA allows the gyrase to wrap DNA around itself and catalyze the supercoiling reaction. The function of DNA gyrase has been correlated to the presence in the CTD of a highly conserved gyrase-specific motif called the 'GyrA-box' (Ward & Newton, 1997). To date, three structures of DNA gyrase CTD have been determined [from *Borrelia burgdorferi* (Corbett *et al.*, 2004), *Escherichia coli* (Ruthenburg *et al.*, 2005) and *Xanthomonas campestris* (Hsieh *et al.*, 2010)]. They all adopt a six-bladed β-pinwheel fold, but display different shapes of the pinwheel. The *E. coli* and *X. campestris* DNA gyrase CTDs adopt a spiral-shaped pinwheel, whereas the *B. burgdorferi* CTD adopts a flat-shaped pinwheel. This underlines the variability in the DNA-wrapping mechanism of DNA gyrase CTDs.

In *Mycobacterium tuberculosis*, DNA gyrase is the sole type II topoisomerase and is therefore the only type II topoisomerase that ensures the regulation of DNA superhelical density (Cole *et al.*, 1998); it is also the sole target of the fluoroquinolones, which are key

antibiotics in the treatment of drug-resistant tuberculosis. As a result, the *M. tuberculosis* enzyme exhibits a different activity spectrum compared with other DNA gyrases, *e.g.* it supercoils DNA with an efficiency comparable to those of other DNA gyrases but shows enhanced relaxation, DNA-cleavage and decatenation activities (Aubry *et al.*, 2006). In order to establish the molecular basis of the specific features of *M. tuberculosis* DNA gyrase, we have solved the structures of the subunit B Toprim and subunit A BRD domains (Piton *et al.*, 2009, 2010). These structures allowed us to identify two important structural specific motifs which could be correlated with the wider substrate spectrum of *M. tuberculosis* DNA gyrase function (Piton *et al.*, 2010).

To provide further structural data with regard to the specific features of *M. tuberculosis* DNA gyrase, we have crystallized and performed X-ray crystallographic studies of the CTD in order to investigate the role of this domain in these specific features. This is the first report of the crystallization and preliminary X-ray diffraction studies of a DNA gyrase CTD from a species containing one unique type II topoisomerase.

2. Materials and methods

2.1. Cloning, protein production and purification

The gene encoding the *M. tuberculosis* DNA gyrase CTD (residues 512–838 of subunit A) was amplified from genomic DNA of *M. tuberculosis* strain H37Rv by polymerase chain reaction (PCR) using specific primers. The forward primer (5′-TTT TTT **TCC ATG G**CC CGC GAG GAC GTC GTT GTC ACT-3′) contained an *Nco*I restriction site (bold), while the reverse primer (5′-TTT TTT **AAG CTT** *TTA* ATT GCC CGT CTG GTC TGC GCC-3′) contained a *Hin*dIII site (bold). The PCR product was then cloned between the *Nco*I and the *Hin*dIII sites of the pET-M11 vector (derived from the pET-28a vector; Novagen, USA). This construct contains an additional hexahistidine tag at the N-terminus followed by a tobacco etch virus protease (TEV) cleavage site. The recombinant plasmid was transformed into *E. coli* BL21 (DE3) pLysS strain (Novagen) and the cells were grown in a shaking incubator at 310 K in LB broth medium supplemented with 50 µg ml^{-1} kanamycin and 40 µg ml^{-1} chloramphenicol. Protein expression was induced by adding 1 m*M* IPTG when the cells reached an optical density at 600 nm of about 0.7. The cells were cultured for an additional 4 h and were harvested by centrifugation at 7000*g* for 30 min at 277 K. The cell pellet was resuspended in binding buffer (50 m*M* Tris pH 8.0, 200 m*M* NaCl, 10 m*M* imidazole) and sonicated at 277 K. The crude lysate was centrifugated at 17 000*g* for 1 h at 277 K. The supernatant was first filtrated using Millex-GV 0.22 µm filters (Millipore) and then loaded onto a pre-equilibrated (with binding buffer) Ni^{2+}-chelating HisTrap HP column (GE Healthcare, USA). The protein was eluted with 50 m*M* Tris pH 8.0, 200 m*M* NaCl and 300 m*M* imidazole. The fractions containing the CTD were pooled, dialysed overnight at 277 K against 50 m*M* Tris pH 8.0 and concentrated at 277 K using Vivapore 10 filters (Sartorius). The His tag was cleaved overnight at 277 K using TEV protease at a molar ratio of 1:50. The cleaved CTD protein was loaded onto the same pre-equilibrated HisTrap HP column. The flowthrough containing the cleaved CTD was loaded onto a HiTrap Heparin HP column (GE Healthcare, USA) pre-equilibrated with Tris pH 8.0, 200 m*M* NaCl. The protein was eluted with Tris pH 8.0, 2 *M* NaCl. The fractions containing the CTD protein were pooled, concentrated and further purified by size-exclusion chromatography on a Superdex 75 10/30 column (GE Healthcare, USA) pre-equilibrated with 50 m*M* Tris pH 8.0, 300 m*M* NaCl. The purified protein was concentrated to 15 mg ml^{-1}; its purity was examined by 12% SDS–PAGE and it was determined to be >95% pure.

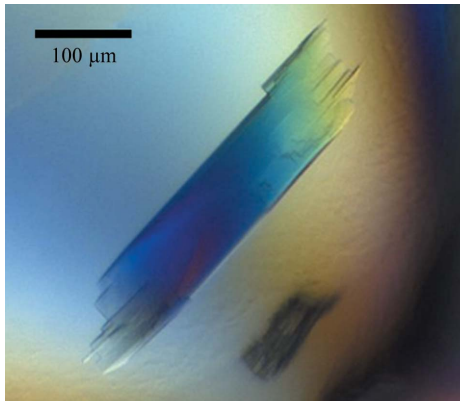

Figure 1
Crystal of the *M. tuberculosis* DNA gyrase CTD grown using 0.1 *M* HEPES pH 7.5, 0.2 *M* sodium chloride, 20%(*v*/*v*) PEG 3000 with a protein concentration of 15 mg ml^{-1}. After 1 d, the crystal dimensions were 100 × 200 × 600 µm.

2.2. Crystallization and data collection

Crystallization of the CTD was initiated by crystallization screening (600 conditions) at 293 K using the hanging-drop vapour-diffusion method in 96-well Greiner plates. Drops consisting of 100 nl protein solution in size-exclusion buffer and 100 nl reservoir solution were dispensed using a Mosquito robot (TTP LabTech) and were equilibrated against 100 µl reservoir solution. Initial crystallization trials were performed using several commercial screening kits: Crystal Screen, Crystal Screen 2, PEG/Ion and Crystal Screen Cryo from Hampton Research, Wizard I and II and JBS 1–8 from Jena Biosciences, and MDL I and II from Molecular Dimensions. Preliminary screening performed at 293 K with a 1:1 mixture of protein solution (15 mg ml^{-1}) and 0.1 *M* HEPES pH 7.5, 0.2 *M* sodium chloride, 20%(*v*/*v*) PEG 3000 (condition No. 28 of Wizard I from Jena Biosciences) gave plate-shaped crystals (Fig. 1). The most suitable-sized crystal was flash-cooled after soaking in a Paratone-N oil/paraffin mixture for 3 s. The initial crystallization condition was reproduced and was further optimized by varying the protein concentration (from 6 to 20 mg ml^{-1}), the pH and the nature and the concentration of the salt. The optimal crystallization conditions were obtained at 293 K and consisted of 20–30%(*v*/*v*) PEG 3350, 0.1 *M* HEPES pH 7.5, 0.1 *M* NaCl using 1 µl 15 mg ml^{-1} protein solution mixed with 1 µl reservoir solution. Each hanging drop was equilibrated against 1 ml reservoir solution. Suitable-sized crystals were obtained after microseeding. After soaking for 3 s in a cryoprotectant solution consisting of 0.1 *M* HEPES pH 7.5, 0.2 *M* sodium chloride, 40%(*v*/*v*) PEG 3350, the crystals were flash-cooled in liquid nitrogen. Crystals obtained from the screening experiment and those obtained in the optimized screens were used for data collection.

X-ray diffraction data were collected at 100 K on beamline PROXIMA 1 at the SOLEIL synchrotron, Saint-Aubin, France using an ADSC Quantum 315 CCD detector. A total rotation range of 120° was covered with 0.5° oscillation and 0.2 s exposure per frame. The wavelength of the incident beam was 0.98 Å and the crystal-to-detector distance was set to 219 mm. X-ray diffraction data were collected to about 1.5 Å resolution. Data were processed with *XDS* (Kabsch, 2010) and scaled with *SCALA* (Evans, 2006) from the *CCP*4 suite (Winn *et al.*, 2011). Molecular replacement was performed with *AMoRe* (Navaza, 1994) using the structure of the *B. burgdorferi*

Table 1
Data-collection statistics.

Beamline	SOLEIL PROXIMA 1
Wavelength (Å)	0.98
Resolution range (Å)	40.50–1.55 (1.63–1.55)
Space group	$P2_12_12_1$
Unit-cell parameters (Å)	a = 38.1, b = 79.7, c = 86.8
No. of unique reflections	41076 (1375)
Mutiplicity	4.5 (3.6)
Completeness (%)	99.0 (95.3)
Molecules per asymmetric unit	1
V_M (Å^3 Da^{-1})	1.85
Solvent content (%)	33.6
$\langle I/\sigma(I)\rangle$	10.3 (2.2)
R_{merge}† (%)	8.6 (53.1)

† $R_{merge} = \sum_{hkl}\sum_i |I_i(hkl) - \langle I(hkl)\rangle| / \sum_{hkl}\sum_i I_i(hkl)$, where $I_i(hkl)$ is the intensity of the ith observation of reflection hkl and $\langle I(hkl)\rangle$ is its mean value.

DNA gyrase CTD (PDB entry 1suu; Corbett *et al.*, 2004), which crystallizes in the same space group with similar unit-cell parameters to *M. tuberculosis* CTD, and the *E. coli* DNA gyrase CTD (PDB entry 1zi0; Ruthenburg *et al.*, 2005) as search models.

3. Results and discussion

The *M. tuberculosis* DNA gyrase CTD (amino acids 512–838 of subunit A) was cloned, overexpressed, purified and crystallized for structural studies. High-throughput crystallization screening was first performed using the His-tagged protein and gave no crystals, whereas the cleaved protein led to several crystallization hits within a day. The selected crystal obtained in the initial screening experiment and those obtained in the optimized screens gave high-resolution diffraction data to about 1.5 Å resolution.

The crystals belonged to space group $P2_12_12_1$, with unit-cell parameters a = 38.1, b = 79.7, c = 86.8 Å. Data-collection statistics are provided in Table 1. Matthews coefficient calculations (Matthews, 1968) suggested that the asymmetric unit contains one molecule, with a V_M of 1.85 Å^3 Da^{-1} and a solvent content of 33.6%. The low solvent content could explain why the His-tagged CTD protein did not crystallize under the conditions explored. Therefore, cleavage of the His tag is a crucial step in obtaining high-quality diffracting crystals of the *M. tuberculosis* DNA gyrase CTD.

Surprisingly, molecular replacement using the *B. burgdorferi* DNA gyrase CTD (PDB entry 1suu) as the starting model gave no solution despite having similar unit-cell parameters in space group $P2_12_12_1$. In contrast, phases could be determined by molecular replacement using the *E. coli* DNA gyrase CTD (PDB entry 1zi0). The best molecular-replacement solution showed good crystal packing without any steric clashes between symmetric molecules. Using phases calculated from this solution, automated model building was performed using *ARP*/*wARP* (Langer *et al.*, 2008) and built more than 97% of the complete model. Initial refinement gave R_{work} = 42.6% (R_{free} = 43.9%). The final model is currently being refined.

We would like to thank Ahmed Haouz of the Crystallogenesis Platform at the Institut Pasteur and the local contact of the beamline PROXIMA 1 at SOLEIL (Saint-Aubin). This work was supported by grants from Région Ile-de-France. We thank Olivier Poch for helpful discussions.

References

Aubry, A., Fisher, L. M., Jarlier, V. & Cambau, E. (2006). *Biochem. Biophys. Res. Commun.* **348**, 158–165.
Champoux, J. J. (2001). *Annu. Rev. Biochem.* **70**, 369–413.
Cole, S. T. *et al.* (1998). *Nature (London)*, **393**, 537–544.
Corbett, K. D., Shultzaberger, R. K. & Berger, J. M. (2004). *Proc. Natl Acad. Sci. USA*, **101**, 7293–7298.
Evans, P. (2006). *Acta Cryst.* D**62**, 72–82.
Forterre, P. & Gadelle, D. (2009). *Nucleic Acids Res.* **37**, 679–692.
Hsieh, T.-J., Yen, T.-J., Lin, T.-S., Chang, H.-T., Huang, S.-Y., Hsu, C.-H., Farh, L. & Chan, N.-L. (2010). *Nucleic Acids Res.* **38**, 4173–4181.
Kabsch, W. (2010). *Acta Cryst.* D**66**, 125–132.
Kampranis, S. C. & Maxwell, A. (1996). *Proc. Natl Acad. Sci. USA*, **93**, 14416–14421.
Langer, G., Cohen, S. X., Lamzin, V. S. & Perrakis, A. (2008). *Nature Protoc.* **3**, 1171–1179.
Levine, C., Hiasa, H. & Marians, K. J. (1998). *Biochem. Biophys. Acta*, **1400**, 29–43.
Matthews, B. W. (1968). *J. Mol. Biol.* **33**, 491–497.
Navaza, J. (1994). *Acta Cryst.* A**50**, 157–163.
Piton, J., Matrat, S., Petrella, S., Jarlier, V., Aubry, A. & Mayer, C. (2009). *Acta Cryst.* F**65**, 1182–1186.
Piton, J., Petrella, S., Delarue, M., Andre-Leroux, G., Jarlier, V., Aubry, A. & Mayer, C. (2010). *PLoS One*, **5**, e12245.
Ruthenburg, A. J., Graybosch, D. M., Huetsch, J. C. & Verdine, G. L. (2005). *J. Biol. Chem.* **280**, 26177–26184.
Schoeffler, A. J. & Berger, J. M. (2008). *Q. Rev. Biophys.* **41**, 41–101.
Ward, D. & Newton, A. (1997). *Mol. Microbiol.* **26**, 897–910.
Winn, M. D. *et al.* (2011). *Acta Cryst.* D**67**, 235–242.